

Intermittency and period-doubling cascade on tori in a bimode laser model

Christophe Letellier^{a,*}, Mounia Bennoud^b, Gilles Martel^b

^a *Groupe d'Analyse Topologique et de Modélisation de Systèmes Dynamiques, CORIA UMR 6614, Université de Rouen, Av. de l'Université, BP12, F-76801 Saint-Etienne du Rouvray Cedex, France*

^b *Groupe d'Optique et d'Optronique, CORIA UMR 6614, Université de Rouen, Av. de l'Université, BP12, F-76801 Saint-Etienne du Rouvray Cedex, France*

Accepted 13 January 2006

Abstract

Dynamical regimes observed in a bipolarized neodymium-doped fibre laser self Q -switched by a thin slice of a polymer-based saturable absorber were recently reported [Martel G, Bennoud M, Ortac B, Chartier T, Nunzi J-M, Boudebs G, et al. Dynamics of a vectorial neodymium-doped fibre laser passively Q switched by a polymer-based saturable absorber. *J Modern Opt* 2004;51(1):85–95]. Among them, period-doubling cascade, chaotic and intermittent regimes have been identified but due to the shortness of the time series available, it was not possible to investigate them with the techniques of the nonlinear dynamical system theory. With the help of a rate-equation based bimode laser model, a period-doubling cascade on tori and intermittent behaviors with underlying torus-like structure are investigated.

© 2006 Elsevier Ltd. All rights reserved.

1. Introduction

During the last decades, the nonlinear dynamical system theory introduced various techniques for characterizing aperiodic regimes [2,3]. These techniques can be applied to dynamical systems belonging to very different areas like physics, chemistry or biology. One of the interesting aspects of these studies is to classify the different regimes observed and to evidence some kinds of universal routes to chaos. Thus, the period-doubling cascade and the three types of intermittencies have been observed in many various situations. All of them have been observed in laser systems. For instance, a period-doubling cascade [4], type-I [5] and type-III intermittencies [6,7] as well as the Lorenz type of chaos [8] have been observed in an optically pumped NH_3 laser systems. Type-II intermittencies have been observed in a GaAs/GaAlAs semiconductor laser [9] and in a driven laser with a saturable absorber [10]. There is another route to chaos, more rarely observed, which consists in a period-doubling cascade of torus [11–15]. This route to chaos has been identified [16] in the Zeghlache–Mandel equations for a detuned laser [17].

Recently, period-doubling cascade and intermittent behaviors were observed in a bipolarized neodymium-doped fibre laser self Q switched by a thin slice of a polymer-based saturable absorber [1]. Unfortunately, the experimental

* Corresponding author.

E-mail address: christophe.letellier@coria.fr (C. Letellier).

set-up did not allow to record sufficiently long time series for clearly identifying the intermittent behavior. Thus, a bimodel laser model based on coupled-cavity atomic rate equations proposed by Bielański et al. [18] is used to investigate in details different typical dynamics. This model is sufficiently accurate to describe the experimental laser investigated in [1] to expect a correspondence between the simulated and the observed behaviors.

Indeed, bipolarized eigenmodes of a fibre laser are multiple in essence [19]. Short time fluctuations are unavoidable in such lasers. They require to average any phase-coupling effects and the significant variable becomes the total intensity of each polarization mode. Thereby, a rate-equation model appears to be a sufficiently rigorous model in this case since no evidence of any such coupling effect through the saturable absorber has been observed for the two polarized modes in our experiments [1]. But note that in the case where two independent lasers are coupled by a common intra-cavity saturable absorber [20–22], perturbed burst oscillations can be observed depending on the relative phase between them. Thus, the intra-cavity saturable absorber medium is simply modeled as an in-intensity dependent nonlinear element with similar saturation coefficients for the two modes. It means that factors C and D in the theoretical model by [20–22] are equals to unity in the model described in this paper. It is not easy to know whether such a simplification which restricts the number of free parameters—perhaps difficult to estimate experimentally [21]—limits the variety of the observable dynamical regimes.

In this paper, we will mainly focus our attention on two different types of regimes, namely intermitencies superimposed to a torus-like structure and a period-doubling cascade on tori. In Section 2 the experimental set-up is briefly described. The corresponding model is discussed in Section 3 and its dynamical analysis is detailed in Section 4. Section 5 is a conclusion.

2. Experimental configuration for a bipolarized fibre laser

The sketch of the experimental set-up is shown in Fig. 1 and is detailed in [1]. For completion let us describe its main characteristics. The pump laser diode (LD) delivers a stabilized and linearly polarized 150 mW output beam at $\lambda_p = 810$ nm. It is isolated from any optical feedback with an optical Faraday isolator (OFI) with an extinction ratio: 40 dB. A half-wave plate (HWp) at λ_p allows to rotate the pump polarization. The laser oscillates at $\lambda = 1.08$ μm (neodymium doped fibre) in a standard linear Fabry–Perot cavity arrangement. In order to allow modulation of the cavity by the saturable absorber it is necessary to focus the intracavity beam using two microscope lenses ($mo_{3,4}$). The saturable absorber (SA) is made up of a thin slice (≈ 3 – 5 μm) of organic dye deposited on a microscope glass plate [23] and is inserted at the focal plane of the unity-magnified intracavity telescope ($mo_{3,4}$). The saturable absorber is inserted between one end of the fibre and its collimating microscope objective ($mo_{1,2}$) to allow self Q -switch. Although such configuration eliminates the intracavity telescope it has appeared less stable and less easy to use for identifying the pertinent regimes and the route to chaos.

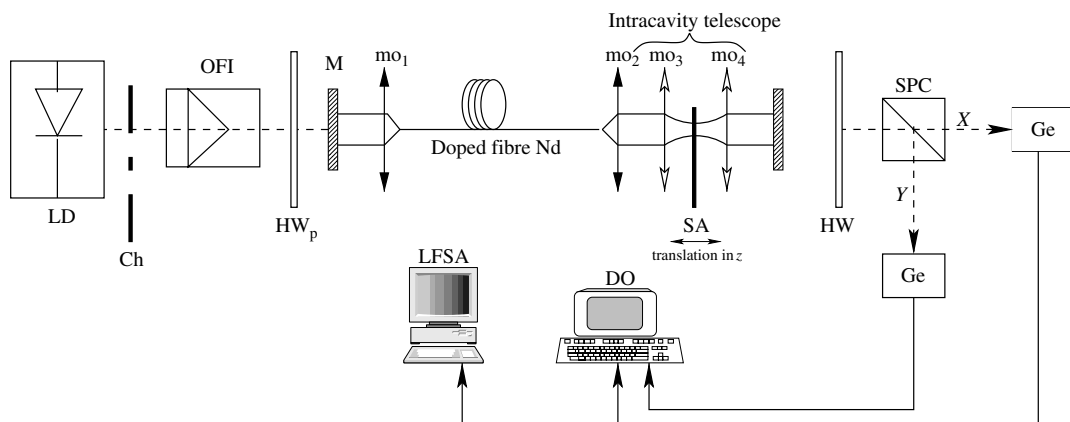


Fig. 1. Experimental set-up. Elements not described in the text are DO, digitizing oscilloscope (BandPass = 600 MHz); LFSA, low frequency spectrum analyzer; HW, half-wave plate at 1.08 μm ; SPC, separator polarization cube; Ge, germanium fast photodiodes; and Ch, chopper.

3. Model

In order to simulate dynamics similar to the regime observed with the previous set-up, we start from a bimode laser model based on coupled-cavity atomic rate equations, with phenomenological population inversions and pumping parameters [18]. A more fundamental microscopic approach has been proposed [24] few years later. Although these two models involved different formalisms, Chartier et al. [25] have shown that these models are isomorphismic. With the incorporation of additive terms in order to model the internal cavity saturable absorber, the equations modeling our laser can be written in the following adimensional form:

$$\begin{cases} \dot{x}_1 = A - x_1 - (x_2 + \beta y_2)x_1 \\ \dot{x}_2 = \kappa \left(-1 + (x_1 + \beta y_1) - \frac{\alpha}{1 + a(x_2 + y_2)} \right) x_2 \\ \dot{y}_1 = \gamma A - y_1 - (y_2 + \beta x_2)y_1 \\ \dot{y}_2 = \kappa \left(-1 + (y_1 + \beta x_1) - \frac{\alpha}{1 + a(x_2 + y_2)} \right) y_2 \end{cases} \quad (1)$$

Each polarized mode ($1 \equiv X$, $2 \equiv Y$) is described by its normalized intensity I_i and by its normalized population inversion D_i . Assuming that the decay time of the saturable absorber is very short (evaluated around 4 ns in [8]), we have eliminated adiabatically the absorber variable. Time is normalized with respect to the population inversion decay constant. Parameter a represents the ratio between the saturation intensity of the laser and the saturation intensity of the absorber times a factor of 2. Parameter a is assumed to be the same for both polarizations. Literature [23,26] allows to evaluate a around 1.6 for the neodymium-doped fibre laser and BDeN saturable absorber used here. However, global dynamics predicted by Eqs. (1) have revealed themselves to be quasi insensitive to a change in parameter a over the range [0.3;3.0]. This is an interesting result since it allows to develop similar results with other saturable absorber and laser medium. α is the normalized population difference of the absorber without saturation. A is the pumping parameter. γ models the pumping anisotropy induced by the pump half-wave plate (HWp). In the following we have assumed, without loss of generality, $\gamma < 1$. This means that the first laser threshold is for mode X . The same normalized lifetime, κ , has been assumed for both laser fields. β is the cross-saturation coefficient describing how each laser field is coupled with the population inversion of the other laser mode. Its value has been experimentally evaluated from the evolution of the eigenfrequencies of the laser versus the pumping power [18]. Its measured value is about 0.53. Similar developments as those performed in [27] but this time applied to (1) leads to the similar simple formula linking parameter γ , parameter β and the two thresholds for the two modes (${}^1A_{\text{th}} = {}^X A_{\text{th}}$ and ${}^2A_{\text{th}} = {}^Y A_{\text{th}}$):

$$\frac{{}^2A_{\text{th}}}{{}^1A_{\text{th}}} \approx \frac{(1 - \beta)(1 + \gamma)}{2(\gamma - \beta)} \quad (2)$$

For a given experimental position of the pump half-wave plate HWp allowing maximum separation for the two thresholds in intensities, parameter γ has been evaluated around 0.95. Recent analysis on bifurcation diagrams obtained with ion-pair model of erbium-doped fibre laser has revealed the strong influence of parameters β and γ on the route to chaos [28]. Similar strong dependence is revealed also with Eq. (1) as shown below.

Numerical integration of system (1) has been performed with a fourth-order Runge–Kutta method with an adaptive integration step. A typical chaotic behavior is shown in Fig. 2.

For all simulations, we use as initial conditions:

$$\begin{cases} x_1 = \frac{A}{1 + u_1 + \beta u_2} \\ x_2 = 0.01u_1 \\ y_1 = \frac{\gamma A}{1 + u_2 + \beta u_1} \\ y_2 = 0.01u_2 \end{cases}$$

where $u_1 = 0.445013$ and $u_2 = 0.010008$.

Note that system (1) is four-dimensional. Thus, quite complex dynamics can be expected, in the sense that the most powerful techniques for characterizing the topology of chaotic attractors are only valid for three-dimensional systems [3]. Our ability to characterize nonlinear dynamics is thus quite limited and far less documented for higher-dimensional systems.

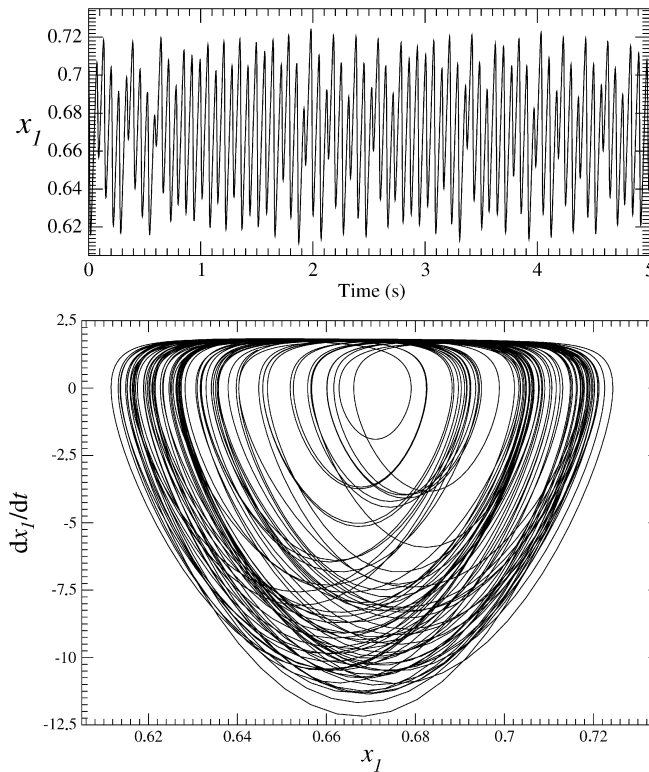


Fig. 2. Typical chaotic behavior of the bimode laser model (1) for $A = 2.5$, $\beta = 0.5$, $\kappa = 5000$, $\gamma = 0.85$, $\alpha = 0.0025$ and $a = 0.8$.

4. Dynamical analysis

4.1. Bifurcation diagram

In order to have a global view of the possible dynamical regimes solution of system (1), a bifurcation diagram is computed using the Poincaré section defined as

$$P \equiv \{(x_{1,n}, y_{1,n}, y_{2,n}) \in \mathbb{R}^3 | \dot{x}_{1,n} = 0, \ddot{x}_{1,n} > 0\} \quad (3)$$

Coordinate $x_{1,n}$ is chosen to compute the diagrams shown in Fig. 3. This bifurcation diagram presents a large period-3 window at the right part of the (bifurcation) diagram. The corresponding period-3 orbit thus significantly structures the dynamical regimes observed. Note that a period-3 limit cycle, not reported in [1], has been recently observed by finely adjust the experimental parameters such as total and anisotropic losses, see [1]. At the extreme right part, an incomplete inverse period-doubling cascade is observed (Fig. 3). A boundary crisis with an unstable orbits (not identified) interrupts the cascade at $A = 2.8074$ (Fig. 3b). Over the interval $A \in [2.8074; 2.904]$, depending on initial conditions, the asymptotic behavior may settle down onto a period-2 limit cycle belonging to the inverse period-doubling cascade or onto a period-3 limit cycle. At the end of the three branches at the lower part of the blow-up of the bifurcation diagram (Fig. 3b), an unusual pattern is observed and is investigated now.

4.2. Period-doubling on the torus

One of the most familiar route to chaos is the period-doubling cascade evidenced by Feigenbaum [29] and Coulet and Tresser [30], independently. Experimental evidences of this cascade have been observed in many situation. Nevertheless, it may appear that the cascade is disrupted or become unobservable due a boundary crisis. As previously mentioned, such a cascade can also occur on tori. One of the most favorable configuration for such a route to chaos is when the system is driven by an external periodic force [11]. In that case, some strong conditions of irrationality between the frequencies involved in the dynamics are required to ensure the existence of quasi-periodic behavior on the torus. A

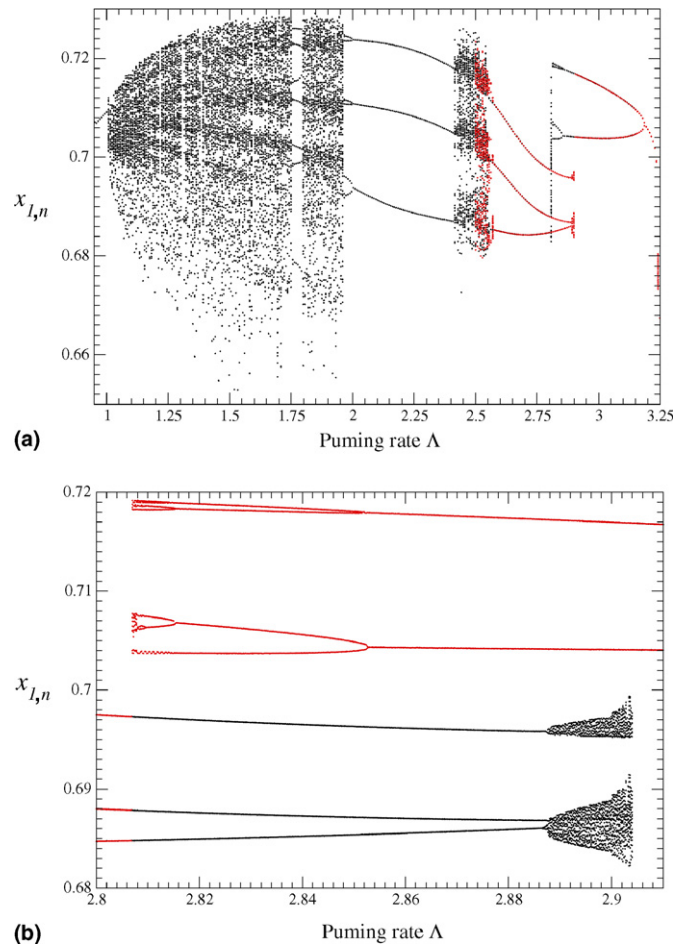


Fig. 3. Bifurcation diagrams of the bimode laser model (1) versus parameter Λ . Parameter values: $\beta = 0.5$, $\kappa = 5000$, $\gamma = 0.85$, $\alpha = 0.0025$ and $a = 0.8$. (a) Bifurcation diagram (b) Blow-up.

recent study has been proposed in the case where a Matsumoto-Chua circuit is driven by a periodic external force [15]. This cascade may be easily avoided when the conditions of irrationality are not exactly set as predicted by Arnéodo et al. [11].

A cascade of period-doublings on tori has been recently observed in an autonomous system left invariant under a continuous rotation symmetry [16]. In such a case, the bifurcations on tori results from the topological product of the limit cycles of the period-doubling cascade by a continuous rotation. The symmetry property of the system are imposed by the existence of a circle of fixed points that is robust against parameter changes.

The bimode laser model (1) is autonomous and has no continuous rotation symmetry. It has a dimension equal to 4 which is the minimum dimension required for a period-doubling cascade on tori as explained below. At the end of the period-3 window, a first-return map to a Poincaré section of the phase portrait (Fig. 4a) reveals that the attractor is a torus (Fig. 4b) for $\Lambda = 2.889$. This means that there is a Hopf bifurcation destabilizing the period-3 limit cycle. Two irrational frequencies are thus involved and the behavior settles down onto a torus, that is, onto a quasi-periodic behavior. When the pumping rate is slightly increased at $\Lambda = 2.9$, the torus section presents a doubled structure (Fig. 4c) looks like a period-2 limit cycle. Let us call such a structure a period-2 torus. Such a Poincaré section without any self-intersection of the trajectory in the phase space is made possible since the phase space is four-dimensional. Otherwise the determinism would have been violated. When Λ is increased again, a period-doubling cascade is observed (Fig. 4d and e) up to an accumulation point beyond which a chaotic behavior is recovered (Fig. 4f) but the underlying torus-like structure is still present. For pumping rate Λ greater than 2.9074, the “chaotic” regime in the torus disappears and the asymptotic behavior is the period-2 limit cycle belonging to the inverse period-doubling cascade (Fig. 3b).

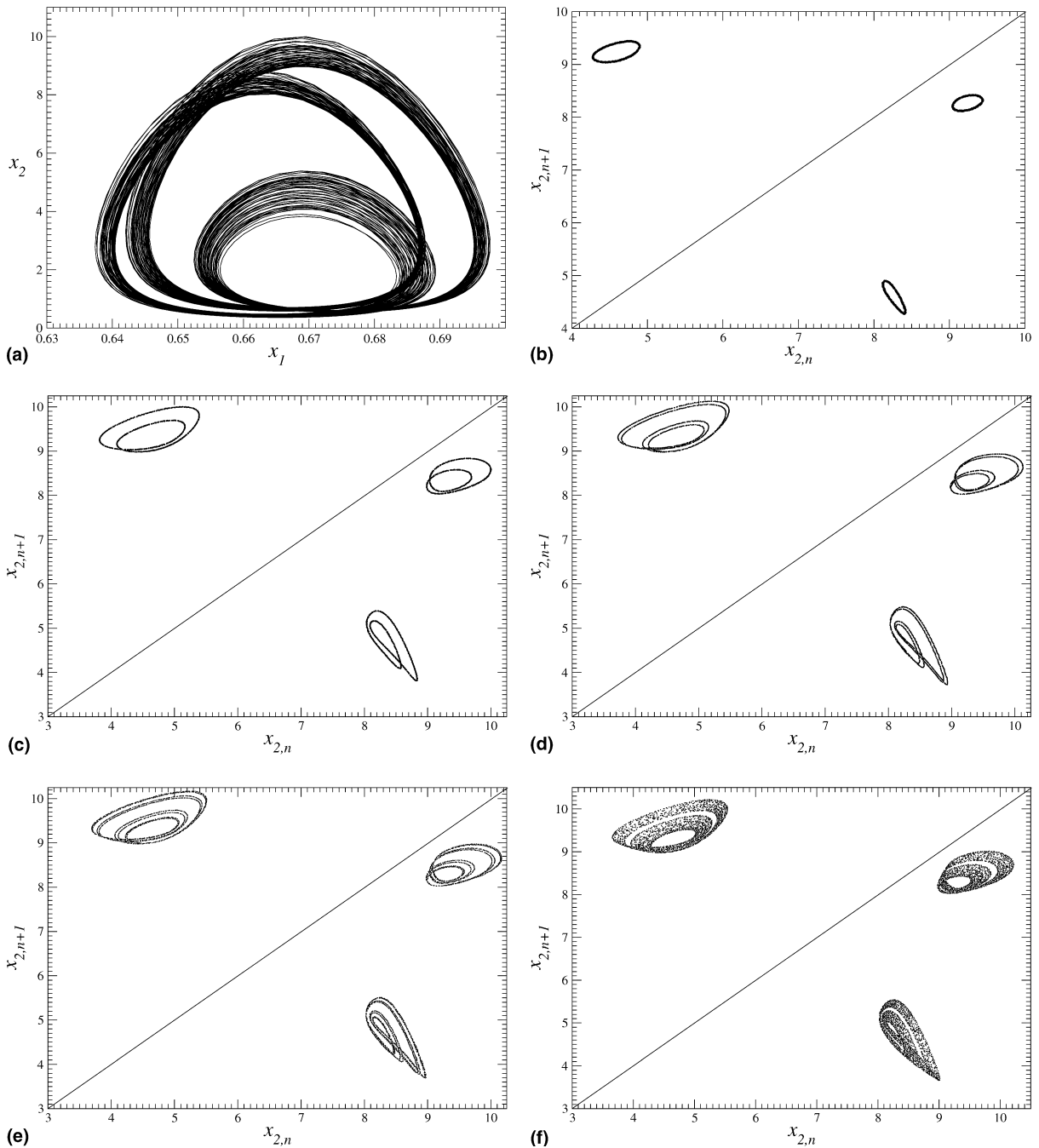


Fig. 4. A quasi-periodic regime (a) for the bimode laser model (1) with $\lambda = 2.889$. Other parameter values are the same as for Fig. 3. First-return map to a Poincaré section P shows three simple “ellipses” (b). Period-2 torus (c), period-4 torus (d), period-8 torus (e) and a chaotic torus (f). (a) Quasi-periodic regime, $\lambda = 2.889$; (b) first-return map, $\lambda = 2.889$; (c) first-return map, $\lambda = 2.9$; (d) first-return map, $\lambda = 2.9011$; (e) first-return map, $\lambda = 2.9014$; (f) first-return map, $\lambda = 2.9017$.

Since we have a period-doubling cascade as a route to chaos, the chaotic attractors must be characterized by a first-return map which has a differentiable maximum between two monotonic branches, that is, a parabola. Thus, the bifurcation diagram should be the same as for the logistic map. In particular, a period-3 window with a type-I intermittency should be identified. This is done for $\lambda = 2.9027$ (Fig. 5a) and the intermittency expected just before the periodic

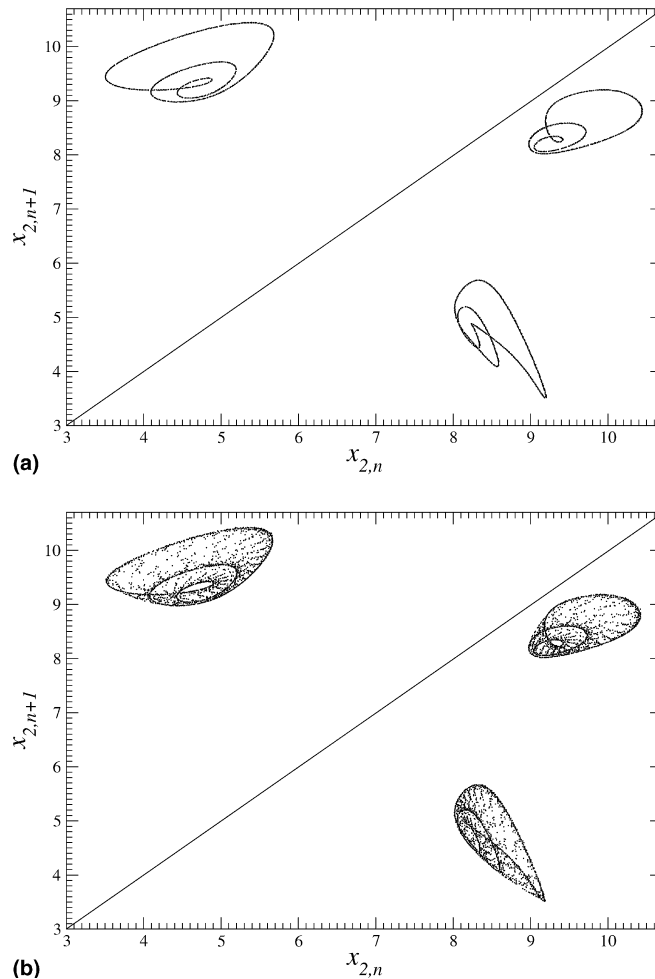


Fig. 5. First-return map to a Poincaré section for the bimode laser model with $\beta = 0.5$, $\kappa = 5000$, $\alpha = 0.005$, $\gamma = 0.85$ and $a = 0.8$. (a) Period-3 window: $A = 2.9027$. (b) Type-I intermittency: $A = 2.902666$.

window is obtained for $A = 0.2902666$ (Fig. 5b). The trajectory thus visits the ghost orbit to be created through a saddle-node bifurcation during long “laminar phases”. This is why the period-3 limit cycle is easily identified in the first-return map shown in Fig. 5b.

A time series of the “intermittent” behavior in the torus is shown in Fig. 6. The period-3 limit cycle appears as the three different sets of maxima. The modulation in the amplitude is due to the visit of the torus-like structure.

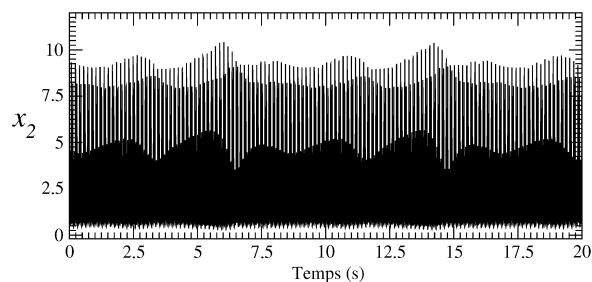


Fig. 6. Time series of the bimode laser model for the type-I intermittency on the torus. Parameter values: $\beta = 0.5$, $\kappa = 5000$, $\alpha = 0.005$, $\gamma = 0.85$, $a = 0.8$ and $A = 2.902666$.

Unfortunately, there is no obvious difference in the time series between the period-3 limit cycle and the intermittent regime in the torus. It is therefore rather difficult to distinguish the laminar phases from the chaotic bursts. Indeed, it is almost impossible to identify such type-I intermittency on a torus from a single time series.

4.3. Intermittency in tori

Among our extended numerical investigations, we found another interesting dynamical regime. For $\alpha = 0.002$ and $\beta = 0.25$, a bifurcation diagram versus parameter a shows an interval over which chaotic behaviors are identified (Fig. 7). The chaotic regime is observed for values of $a \in [1.757675; 1.8085]$. Note that around $a = 1.796$, a period-57 window is observed. Such a high-periodic orbit is identified using a 57th-return map for which the 57 different points are located in the bisecting line. Beyond both sides of this interval, a period-2 limit cycle is observed. As usually observed at the boundary between periodic and chaotic windows, intermittent behaviors are expected. Such intermittency must occur through a tangent bifurcation.

Three types of intermittency have been proposed by Pomeau and Manneville [31]. Type-I intermittency is associated with a saddle-node bifurcation of the limit cycle, type-II intermittency with a subcritical Hopf bifurcation, and type-III with a subcritical period-doubling bifurcation [32]. In the last case, one of the characteristic of type-III intermittency is that the oscillations have typically two components. During laminar phases where the trajectory approaches a ghost orbit to be created, one component grows while the other decreases. Two successive laminar phases are separated by chaotic bursts. Thus, for instance, a type-III intermittency has been observed just after a period-2 window in a NH_3 laser [4]. A type-III intermittency could therefore be expected at both sides of the chaotic window shown in Fig. 7. This is supported by the time series of variable x_2 (Fig. 8) where the two components can be clearly identified.

Nevertheless, in the classical scenario for type-III intermittency, the period-2 limit cycle loses its stability at the tangent bifurcation. Such a bifurcation does not occur in the case of the bimode laser model. In fact, the period-2 limit cycle is still stable and there is a bistability between this cycle and the chaotic behavior shown in Fig. 8. A second-return map to a Poincaré section clearly shows that the period-2 limit cycle is not too close to this chaotic behavior (Fig. 9). The annular shape of the map indicates that this behavior is mainly organized around a torus-like structure which is similar to the section of the torus after the first period-doubling bifurcation (Fig. 4c). Nevertheless, in the present case, this is not related to a period-3 limit cycle as in Fig. 4.

The underlying torus has been identified in varying parameter α . For $\alpha = 0.0021$, there is a quasi-periodic regime (Fig. 10a). Using a second-return map to represent the structure of its Poincaré section helps to evidence that this is a period-2 torus as observed after the first period-doubling bifurcation (Fig. 4c). This already indicates that a four-dimensional system is required to observe such a behavior. This torus is destabilized through a period-doubling bifurcation, and a torus with a section similar to a period-4 limit cycle is observed for $\alpha = 0.00205$ (Fig. 10b). Decreasing again α , some foldings occur on the structure of the torus and for $\alpha = 0.00202$, a three-banded chaotic torus is observed (Fig. 10c). Then, the torus is broken and the intermittent behavior in the torus shown in Fig. 9 is observed.

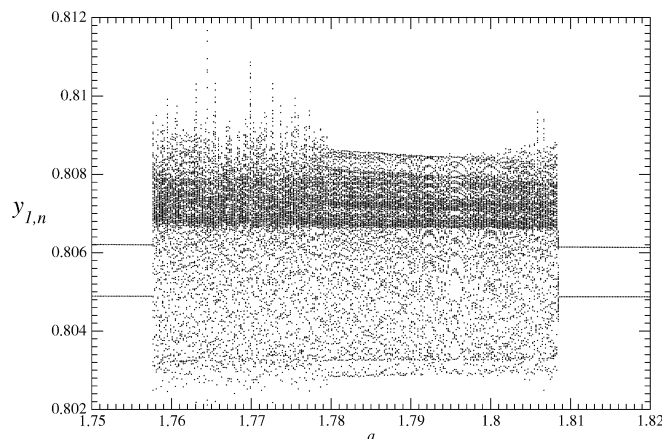


Fig. 7. Bifurcation diagram near the intermittent behavior observed for $\alpha = 0.002$, $\beta = 0.25$, $\kappa = 5000$, $\gamma = 0.85$ and $A = 1.5$.

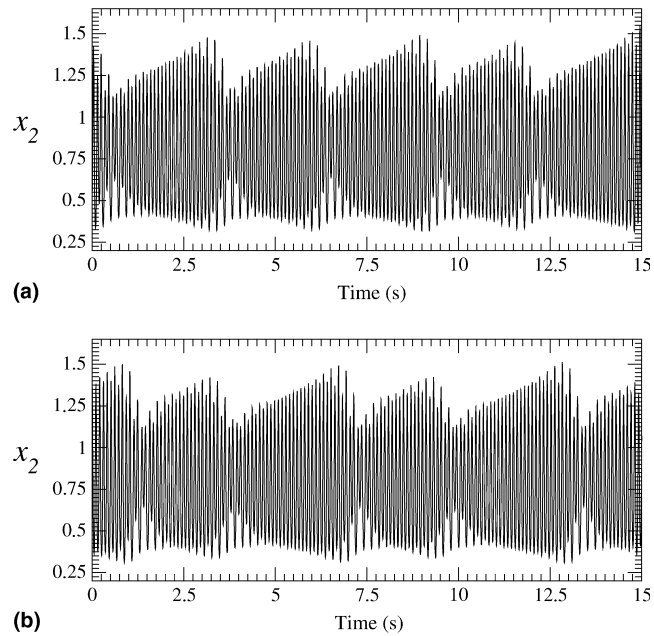


Fig. 8. Time series of variable y_1 of the bimode laser model (1) with $A = 1.5$, $\beta = 0.25$, $\kappa = 5000$, $\gamma = 0.85$ and $\alpha = 0.002$. (a) $a = 1.7576752$ and (b) $a = 1.8085$.

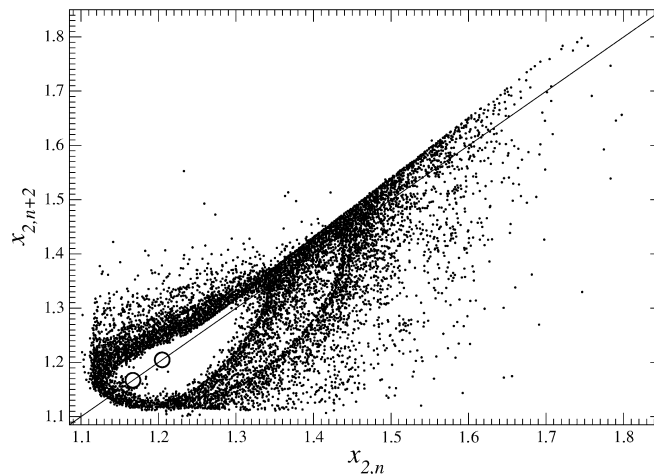


Fig. 9. Second-return map to a Poincaré section with $A = 1.5$, $\beta = 0.25$, $\kappa = 5000$, $\gamma = 0.85$, $\alpha = 0.002$ and $a = 1.757675$. The two periodic points of the stable period-2 limit cycle which co-exists in the phase space are also shown.

The torus breaking occurs through a tangent bifurcation between the torus and the bisecting line. Such a tangent bifurcation is evidenced by using a second-return angular map computed as follows. The barycentre of the second-return map is chosen as the reference point. An angle θ_n is defined for each point of the map shown in Fig. 9 with respect to an horizontal segment, parallel to the abscissa and coming from the barycentre. Then, the angular second-return map is obtained by plotting θ_{n+2} versus θ_n as shown in Fig. 11. The existence of a small channel between this angular map and the bisecting line induces the intermittent behavior.

A Fourier spectrum confirms the fact that the behavior is more complex than a quasi-periodic regime (Fig. 12). If many isolated peaks can be identified, there is also a broadened band of frequencies. A similar Fourier spectra has been experimentally obtained in [1] for intermittent regimes. This is quite typical of a chaotic regime. The superimposition of

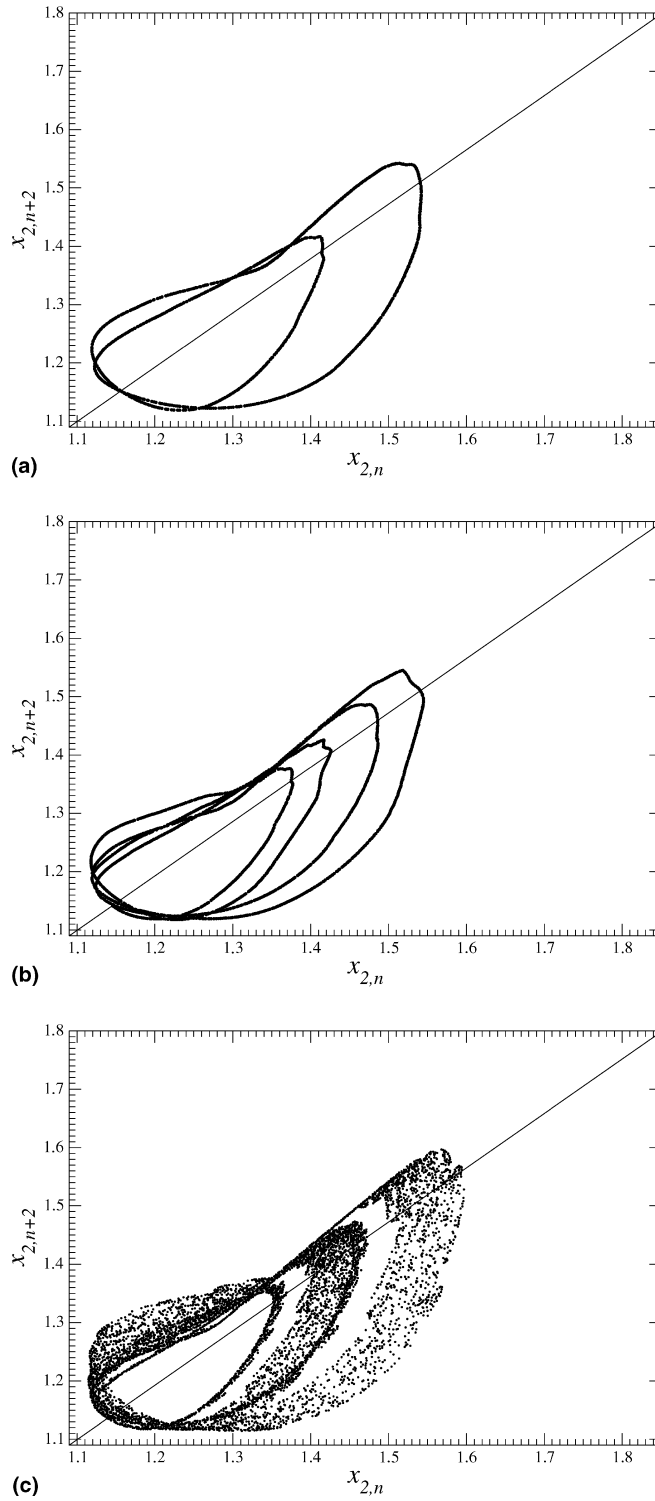


Fig. 10. Second return maps to Poincaré section P for the bimode laser model (1) with the same parameter values as used for Fig. 9. (a) Quasi-period-2 regime, $\alpha = 0.00210$; (b) period-4 regime, $\alpha = 0.00205$; and (c) chaotic regime in the torus, $\alpha = 0.00202$.

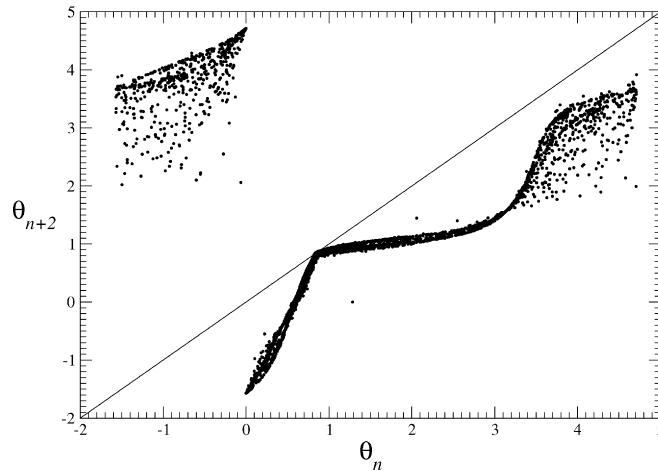


Fig. 11. Angular second-return map to a Poincaré section with $\Lambda = 1.5$, $\beta = 0.25$, $\kappa = 5000$, $\gamma = 0.85$, $\alpha = 0.002$ and $a = 1.75767605$.

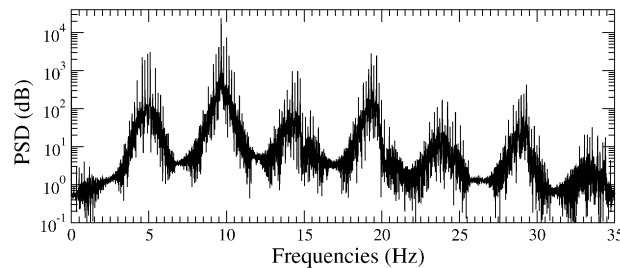


Fig. 12. Fourier spectrum for parameter values: $\Lambda = 1.5$, $\beta = 0.25$, $\kappa = 5000$, $\gamma = 0.85$, $\alpha = 0.002$ and $a = 1.8085$.

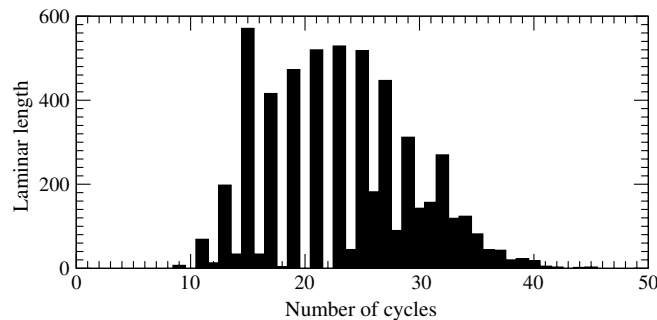


Fig. 13. Distribution of laminar lengths for $\Lambda = 1.5$, $\beta = 0.25$, $\kappa = 5000$, $\gamma = 0.85$, $\alpha = 0.002$ and $a = 1.7576752$.

the isolated peaks and the bands of frequencies is thus a signature of the chaotic regime in the torus. The tangent bifurcation associated with a chaotic behaviors leads us to conclude for an intermittency with an underlying torus-like structure. The usual type-III intermittency cannot occur on a simple torus with an orientable surface [32]. But in the present case, the period-doubling bifurcation on the torus provides a torus with a nonorientable surface. Such a configuration is only possible in a four-dimensional space. This is probably why the time series shown in Fig. 8 have the characteristic of a type-III intermittency, that is, the increase of the sub-harmonic and the related decrease of the fundamental mode [32]. Turbulent bursts occur when the amplitude of the sub-harmonic is roughly equal to the amplitude of the fundamental

mode. Just after, a nearly periodic regime appears again with a sub-harmonic having an arbitrary amplitude. The initial amplitude determines the length of the laminar phase. Weaker the initial amplitude is, longer the laminar phase is.

Another important property which helps to distinguish between different types of intermittency is the laminar length distribution. Such a distribution is not conceptually difficult but quite often hard to compute as in the case of the type-I intermittent behavior in the torus discussed in the previous section. In the present case, the laminar phase are identified using the time series shown in Fig. 8a. It has been observed that chaotic bursts occur when at least one maximum of the oscillations is less than 1.15. The obtained distribution of laminar lengths is shown in Fig. 13. The distribution is not exactly the expected one for a type-III intermittency. Instead of the usual shape characterized by a high peak for short laminar phases associated with a long queue toward the long laminar phases, a bell-shape distribution is observed. Note that for quite short laminar phases (less than 25 cycles), the length cannot be odd: this is again a strong signature of the underlying period-2 torus. For longer laminar phases, this becomes possible, at least with the numerical convention we choose for defining them. A long queue for the large laminar phases is observed. This is typical of a type-III intermittency. Consequently, we could conclude that this intermittent behavior with an underlying torus-like structure is quite close to a type-III intermittency.

5. Conclusion

A bimode laser model has been investigated as a guideline for identifying dynamical regimes in a bipolarized neodymium-doped fibre laser self Q switched. This is a four-dimensional autonomous dynamical system. A period-doubling cascade on tori have been identified before a chaotic regime which have a parabola as a first-return map. As predicted by the logistic map, the corresponding type-I intermittency associated with the period-3 window has been identified. The time series for such an intermittency does not allow to directly identify the intermittent behavior.

For another set of parameter values, another type of intermittency, again with an underlying torus-like structure has been observed. Many of its characteristics leads us to make a parallel with a type-III intermittency. This intermittent behavior is observed after two period-doubling bifurcations on tori.

These behaviors can be only observed in a four or higher-dimensional phase space. The bimode laser model has therefore the minimal dimension required for observing these behaviors.

References

- [1] Martel G, Bennoud M, Ortac B, Chartier T, Nunzi J-M, Boudebs G, et al. Dynamics of a vectorial neodymium-doped fibre laser passively Q switched by a polymer-based saturable absorber. *J Modern Opt* 2004;51(1):85–95.
- [2] Abarbanel HDI, Brown R, Sidorowich JJ, Tsimring LSh. The analysis of observed chaotic data in physical systems. *Rev Modern Phys* 1993;65(4):1331–88.
- [3] Gilmore R. Topological analysis of chaotic dynamical systems. *Rev Modern Phys* 1998;70(4):1455–529.
- [4] Tang DY, Pujol J, Weiss CO. Type-iii intermittency of a laser. *Phys Rev A* 1991;44(1):R35–8.
- [5] Tang DY, Li MY, Weiss CO. Laser dynamics of type-I intermittency. *Phys Rev A* 1992;46(1):676–8.
- [6] Pujol J, Arjona M, Corbalán R. Type-III intermittency in a four-level coherently pumped laser. *Phys Rev A* 1993;48(3):2251–5.
- [7] Tang DY, Heckenberg NR, Weiss CO. The optical field of type-III intermittency pulsing in a single mode laser. *Phys Lett A* 1995;202:363–8.
- [8] Weiss CO, Brock J. Evidence for Lorenz-type chaos in a laser. *Phys Rev Lett* 1986;57(22):2804–6.
- [9] Sacher J, Elsässer W, Göbel EO. Intermittency in the coherence collapse of a semiconductor laser with external feedback. *Phys Rev Lett* 1989;63(20):2224–7.
- [10] San-Martin J, Antoranz JC. Type-II intermittency with a double reinjection channel: multintermittency. *Phys Lett A* 1996;219:69–73.
- [11] Arnéodo A, Couillet PH, Spiegel EA. Cascade of period doublings of tori. *Phys Lett A* 1983;94(1):1.
- [12] Iooss G, Los J. Quasigenericity of bifurcations to high dimensional invariant tori for maps. *Commun Math Phys* 1988;119:453–500.
- [13] Basset MR, Hudson JL. Experimental evidence of period-doubling of tori during an electrochemical reaction. *Physica D* 1989;35:289–98.
- [14] Flesseles J-M, Croquette V, Jucquois S. Period-doubling of a torus in a chain of oscillators. *Phys Rev Lett* 1994;72(18):2871–4.
- [15] dos Santos EP, Caldas IL, Baptista MS. Two-frequency torus breakdown in the driven Matsumoto-Chua circuit. In: *ICONNE* 2000.
- [16] Letellier C. Modding out a continuous rotation symmetry for disentangling a laser dynamics. *Int J Bifurc Chaos* 2003;13(6):1573–7.
- [17] Zeghache H, Mandel P. Influence of detuning on the properties of laser equations. *J Opt Soc Am B* 1985;2:18–22.

- [18] Bielawski S, Derozier D, Glorieux P. Antiphase dynamics and polarization effects in the Nd-doped fiber laser. *Phys Rev A* 1992;46:2811–22.
- [19] Chartier T, Sanchez F, Stéphan G. General model for a multimode Nd-doped fiber laser. I: construction of the model. *Appl Phys B* 2000;70:23–31.
- [20] Barsella A, Lepers C, Dangoisse D, Glorieux P, Erneux T. Synchronization of two strongly pulsating CO₂ lasers. *Optic Commun* 1999;165:251–9.
- [21] Susa I, Erneux T, Barsella A, Lepers C, Dangoisse D, Glorieux P. Synchronization through bursting oscillations for two coupled lasers. *Phys Rev A* 2001;63:013815.
- [22] Barsella A, Lepers C. Chaotic lag synchronization and pulse-induced transient chaos in lasers coupled by saturable absorber. *Optic Commun* 2002;205:397–403.
- [23] Nunzi JM, Pfeffer N, Naudin C, Delysse S, Molva E, Marty J, et al. Study of polymers for saturable absorption: application to monolithic Q-switched microlasers. *Nonlinear Opt* 1996;15:243–6.
- [24] Leners R, Stephan G. Rate equation analysis of a multimode bipolarization Nd³⁺ doped fibre laser. *Quantum Semiclass Opt* 1995;7:757–94.
- [25] Chartier T, Sanchez F, Stéphan G. Bipolarized Nd-doped fibre laser: effects of localized and distributed dichroisms. *Quantum Semiclass Opt* 1998;10:79–86.
- [26] Le Flohic M, François PL, Allain JY, Sanchez F, Stéphan G. Dynamics of the transient buildup of emission in neodymium-doped fiber lasers. *Opt Quantum Electron* 1991;27:1910–21.
- [27] Sanchez F, Stéphan G. General analysis of instabilities in erbium-doped fiber lasers. *Phys Rev E* 1996;53:2110–22.
- [28] Besnard P, Ginovart F, Le Boudec P, Sanchez F, Stéphan GM. Experimental and theoretical study of bifurcation diagrams of a dual-wavelength erbium-doped fiber laser. *Optic Commun* 2002;205:187–95.
- [29] Feigenbaum MJ. Quantitative universality for a class of nonlinear transformation. *J Statist Phys* 1978;19(1):25–52.
- [30] Couillet P, Tresser C. Itérations d'endomorphismes et groupe de renormalisation. *J Phys Coll C* 1978;5(39):5–25 [supplément au no 8].
- [31] Pomeau Y, Manneville P. Intermittent transition to turbulence in dissipative dynamical systems. *Commun Math Phys* 1980;74:189–97.
- [32] Bergé P, Pomeau Y, Vidal C. L'ordre dans le chaos [Trans: Order within chaos. New York: Wiley; 1986]. Paris: Hermann; 1984.